International Journal of Mechanical and Materials Engineering (IJMME), Vol.6 (2011), No.1, 109-119

THERMO-VISUAL INVESTIGATION OF A TWO-PHASE CLOSED LOOP THERMOSYPHON

A.K. Mozumder and M.M. Kamal
Department of Mechanical Engineering, Bangladesh University of Engineering and Technology
Dhaka 1000, Bangladesh
Email: aloke@me.buet.ac.bd

Received 19 November 2010, Accepted 13 March 2011

ABSTRACT

An experimental investigation on heat transfer characteristics for an evaporator of a two-phase closed-looped thermosyphon was carried out. Experiments were conducted using three different evaporator surfaces, namely Pin Finned Surface (PFS), Rectangular Finned Surface (RFS) and Plain Surface (PS) with three different working fluids Acetone, Ethanol and Methanol. Bubble generation frequency and bubble density per unit area were estimated. A fan of 40 W capacity was used to know the forced convection effects on condenser for heat flux. The average heat flux can be increased to approximately 150 % by using the condensing fan. The experimental results show that the heat transfer increases by 150 % for Ethanol with respect to Acetone and this value is 30 % with respect to Methanol. It was found that Rectangular Finned Surface (RFS) can transfer about 30% more heat than Plain Surface and approximately 15 % more than Pin Fin surface.

Keywords: Thermosyphon, Phase change and Boiling heat transfer, Forced convection, Bubble generation

NOMENCLATURE

A	Heat transfer area of the evaporator surface (m^2)
cosθ	Power factor
d_b	Bubble generation density ($/cm^2$)
f_b	Bubble generation frequency (*/sec*)
I	Applied current (*Amp*)
PFS	Pin Fin Surface
PS	Plain Surface
q	Heat flux (w/m^2)
q_L	Heat loss (w/m^2)
RFS	Rectangular Fin Surface
V	Applied voltage (*Volt*)
ΔT	Wall superheat (*K*)

1. INTRODUCTION

Modern life is becoming increasingly dependent on sophisticated electronic devices. Advanced features, faster communication and increased portability will be the hallmarks of future electronics. The trend towards miniaturization and increased functionality has numerous challenges for developing compliant and reliable electronic products. The increasing of electronic systems integration requires an improved cooling technology. Thermosyphon cooling is one of the most promising, being capable of dissipating high heat fluxes with minimal temperature differences. Imura et al. (1983) discovered the important advantage of a two phase closed loop thermosyphon which it's critical heat flux was 1.2 – 1.5 times greater than the heat pipe. A thermosyphon successfully implements two-phase liquid cooling by indirect contact with electronics. A two-phase thermosyphon basically consists of an evaporator and a condenser, which are connected through a passage, or a loop. The tube carrying the vapor from the evaporator is called rising tube or forward tube and the other tube connecting the condenser and evaporator is called the return tube or the falling tube. The fluid vaporizes in the evaporator as heat is transferred from the source to the evaporator. The vapor then moves to the condenser through the tubing where it condenses. The released heat is dissipated into the ambient from the condenser and the condensed liquid is returned to the evaporator, thus completing a loop. The density difference between the liquid and vapor creates a pressure head, which drives the flow through the loop and no other driving force is needed.

Many analytical and experimental investigations (Claudio and Dobran, 1988; Yinxue and Chen, 1995; Gross and Hahne, 1985) were performed during the last few decades. Remaswamy et al. (1998) investigated the liquid/vapor space confinement in the evaporator section. Their results showed a negligible effect of space confinement on the performance of the system. Lang et al. (2001) studied the effects of imposed circulation and location of condenser on the performance of a two- phase thermosyphon in a confined space. They reported imposed circulation using a pump that could make the thermosyphon successfully operated even when the condenser was placed below the evaporator in the imposed circulation thermosyphon for each heat input. Gavotti and Polasek (1999) reported a detailed outline of the applicability of loop thermosyphon for the thermal control of electronic equipments. They concluded that loop thermosyphons were able to dissipate heat fluxes from electronic equipments up to a maximum value of 70 W/cm2, depending primarily on the choice of the working fluid. Ghiu et al. (2001) performed visualization study of pool boiling at atmospheric pressure from top-

covered enhanced structures for a dielectric fluorocarbon liquid (PF 5060). The heat transfer performance of the enhanced structures was found to depend weakly on the channel width. The internal evaporation has a significant contribution to the total heat dissipation, especially at low heat fluxes. The two-phase closed loop thermosyphon was investigated by Charles and Kok (1992) with emphasis on the overall performance in transient operation. The control volume approach was the base of a global analysis describing the motion of vapor and liquid phases of the thermosyphon system in one-dimensional equations. It was found that the density ratio of vapor-liquid, dimensionless friction coefficient and water column length determined respectively the overall dynamic behavior characteristics such as response time, damping and oscillation frequency.

Multiple solutions for closed thermosyphon loops were at first found for single- phase, constant area, one-dimensional models by Ramos et al. (1985). Their result was further extended to variable area loops. The phase-change thermosyphon was also considered, first with a finite two-phase zone and then using a sharp interface approximation. For entirely different reasons, multiple solutions were also found in that case. The physical basis for multiple solutions in the two-phase loop was discussed in detail with the aid of a particular example. An experimental study on the heat transfer performance of a two-phase closed thermosyphon together with a simple theoretical analysis for its maximum heat transfer capacity was made (Lee and Mital, 19972; Hasanuzzaman et al., 2007). Water and Freon-11 were used as the working fluids. Out of many possible controlling variables, the effects of the amount of working fluid in the tube, the ratio of heated-length to cooled length, the operating pressure, the heat flux and the working fluid were investigated.

Mark et al. described the modeling, design, and testing of a high flux and yet compact two-phase CPU cooler, with excellent attributes of low thermal resistance that were derived from the intrinsic design features of phase change phenomena and minimal vapor pressure drop of the device. Testing was conducted over an assorted heat loads and air flow rates flowing through the fins, achieving a best performance of 0.206 K/W of device thermal resistance at a rating of 203 W under an air flow rate of 0.98 m^3/min. The prototype device was orientation free where a 90° tilt could perform at the same rating conditions. A 1-D/2-D model was proposed by Bernier and Baliga for closed-loop thermosyphons with vertical heat transfer sections. This model improved the results of traditional 1-D models for cases where: (i) mixed-convection effects were important in the heated and cooled sections of the loop; and (ii) heat losses (or gains) from the insulated portions of the loop were significant. This was achieved by iteratively coupling local results of 2-D numerical simulations of mixed-convection flows, performed in the heated and cooled sections, and a 1-D analysis. The proposed 1-D/2-D model was validated by comparing its results with those of a complementary experimental study. The aim of the work conducted by Fichera and Pagano (2002) was to address the problem of modeling the dynamical behaviour, manifested during unstable operation, of an experimental closed loop thermosyphon. A generalised Nonlinear Auto-Regressive Moving Average with eXogenous inputs (NARMAX) model, implemented by means of neural networks, was used to address the identification of the system dynamics by means of input–output experimental measurements. An open horizontal heat pipe consisting of a condenser, an adiabatic section, and an evaporator was used to study boiling of R-11 on a surface covered with a porous wick by Mughal and Plumb. Porous metal wicks having two different thicknesses and with and without channels cut in their surfaces were examined. For these types of surfaces the heat flux increased very dramatically with increased in excess temperature once boiling was initiated.

Pin Finned Surface (PFS), Rectangular Finned Surface (RFS) and Plain Surface (PS) with three different working fluids acetone, ethanol and methanol are used in this study. The present study performs the experimental investigation for the effects of the working fluids on heat flux, assessment of the bubble generation frequency and bubble density per unit area and comparing the heat fluxes for different geometries.

2. EXPERIMENTAL SETUP AND PROCEDURE

2.1 Experimental Setup

The schematic diagram of the experimental setup is shown in Fig. 1, which mainly consists of loop thermosyphon (evaporator, condenser and copper tubing), heat supply system, and measurement systems. A digital video camera is used for recording boiling phenomena and a fan is used for producing forced convection heat transfer. Three different working fluids are also used to transport heat from evaporator to condenser.

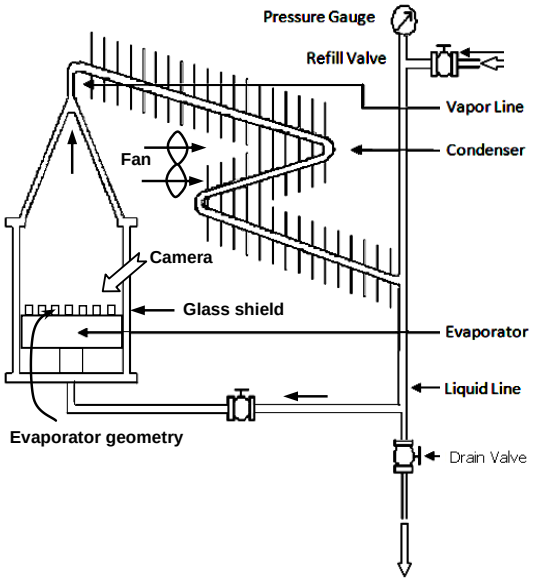

Fig. 1: Schematic diagram of the thermosyphon

Evaporator Section: The boiling chamber was made of 4 mm thick transparent glass tube for clear visualization, the inner diameter of the chamber was 100 mm and length of 120 mm. Two mild steel flanges are fixed on both sides of the glass tube. Proper fittings and provisions are there so that liquid cannot leak out of it and boiling can be observed clearly. It has one vapor outlet with conical shaped chimney and a condensate liquid inlet port. All the body of the evaporator section is properly insulated with gasket. Two thermocouples are embedded inside the enclosure to measure the temperature of boiling liquid and vapor.

Condenser Section: Tube-in-fin type condenser is used and the line diagram of it is shown in Fig. 1. It is cooled by air without fan in free convection mode of heat transfer. A fan is attached in front of the condenser for creating forced convection. 21 Copper fins (30 mm x 30 mm x 1.0 mm thickness) are fixed to a bend copper tube (6 mm ID and 1.0 mm thick at 10 mm spacing) for making the condenser section.

Copper Tubing: It mainly consists of condensate line. Three valves are fixed in the whole system. One is after condenser for filling the fluid or reflux the condenser and next one is under side of the system for drain out the fluid when needed. Another one is placed before the evaporator inlet. A pressure gauge (range from 1 psig to 30 psig) is attached to the loop near the exit of the condenser to monitor the loop pressure.

Evaporator Surface: Three types of evaporator surfaces are experimented in this study. These are evaporator with plain surface (PS), evaporator with pin fins (PFS) and evaporator with integrated rectangular fins (RFS). All the surfaces are of similar dimension and of same material. The differences are in enhanced geometry.

2.2 Experimental Procedure

Before starting the experiment the whole piping system is examined for leak proof at pressurized condition. When it is confirmed that the system is fully leak proof, the setup is ready for the experiment. Then the half volume of evaporator is charged with the relevant fluid and a high heat flux is provided to the heater (about 250 W) with electric means. From the power source, initially 90 V was applied. Then gradually it is increased to 240 V with an interval of 5 V to obtain different evaporator temperatures. After achieving the steady state condition, boiling temperature of the liquid, temperature of the evaporator surface, voltage and current reading were recorded carefully. At the same time a video camera was employed to capture the bubble generating characteristics. From the video images, the bubble generating frequency, f_b and bubble density per unit area, d_b were estimated for evaporator surface of temperature 80^0C, 83^0C and 86^0C. The fan attached to the condenser, is also switched on to observe the effects of forced convection on bubbles generation characteristics. It is observed that pressure remains constant most of the time during the experiment (14 psig), but fluctuation of pressure are also observed at times which is ± 5%. The test is continued until the surface temperature is exceeded 86^0C (a maximum limit for most commercial electronics) for each working fluid. Again for each experimental run, similar arrangements are taken. For particular working fluid and condition, each set of data was recorded. In every step, the temperatures were monitored continuously and the heat input incremented after the system reached steady state. When temperature rise 0.1^0C in a span of 10 minutes or thermometer shows lessen the temperature then reading is taken.

Heat flux is calculated using the following equation:

$$q = (VI\cos\theta - q_L)/A$$

Experiments were conducted using three different evaporator surfaces, namely Pin Finned Surface (PFS), Rectangular Finned Surface (RFS) and Plain Surface (PS) with three different working fluids Acetone, Ethanol and Methanol. The experimental conditions are summarized in Table 1.

Table 1 Experimental conditions

Experimental Parameters	Value / Types
Working Fluid	Methanol Ethanol Acetone
Surface Material	Copper
Surface Finish	Polished with zero grade emery paper
Boiling Surface	Placed at bottom of the evaporator

3. RESULTS AND DISCUSSIONS

2 Effects of Working Fluids on the Heat Flux with Different Geometries

Boiling curves for Pin Finned Surface (PFS) with Methanol, Ethanol and Acetone are given in Fig. 2(a). From this curve it is found that higher heat flux is obtained for Ethanol.

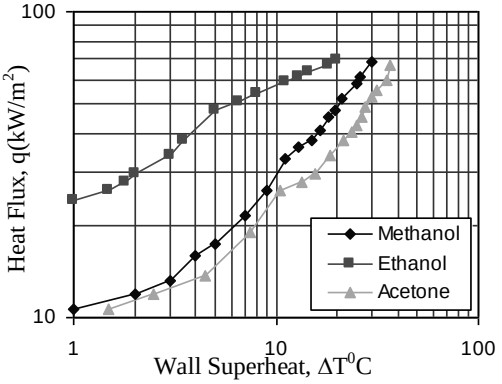

(a) Pin Finned Surface (PFS)

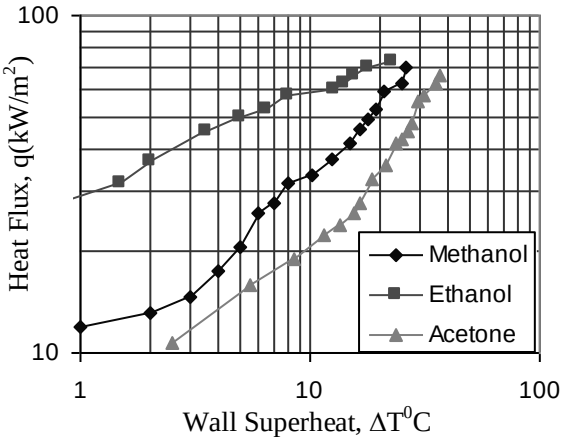

(b) Rectangular Finned Surface (RFS)

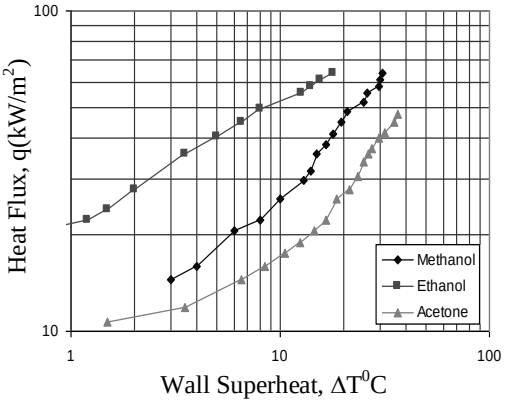

(c) Plain surface (PS)

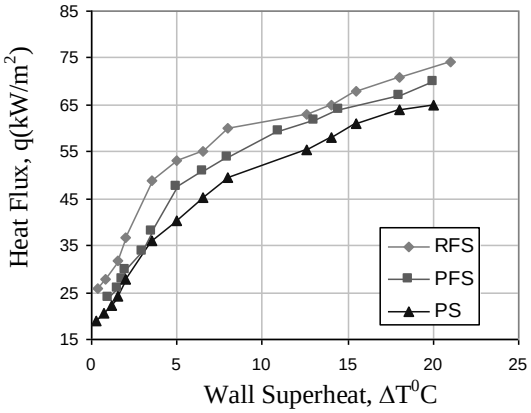

(d) Ethanol with different geometry

Fig. 2 Effects of working fluid and evaporator surface geometry on heat flux

It is to be mention here that Ethanol has the highest boiling temperature (at atmosphere pressure) among all the three fluids which is about 78 ^{o}C (the boiling temperature of Methanol is 64.5 ^{o}C and that of Acetone is 56.3 ^{o}C). For all the fluids heat flux increases with the increase of wall temperature. After 10^{o}C of wall superheat, ΔT, the rate of increase of heat flux with wall superheat increases more rapidly for Methanol and Acetone than Ethanol. This trend shows that at higher wall super heat, the value of heat flux of all the fluids become closer. Immediately just after the wall superheat of 10 ^{o}C, Methanol and Acetone become closer to nucleate boiling region (maximum heat flux region) than Ethanol as the saturation boiling temperature of Methanol and Acetone are lower than that of Ethanol. For this reason, after 10 ^{o}C of wall superheat, the heat flux for Methanol and Acetone increase more rapidly than Ethanol.

Boiling curves for Rectangular Finned Surface (RFS) with Methanol, Ethanol and Acetone are shown in Fig. 2(b). Higher heat flux is also obtained here for Ethanol. Boiling curves for plain surface (PS) with Methanol, Ethanol and Acetone is presented by Fig. 2(c). The heat flux for Ethanol again is the highest here. From Figs. 2(a-c), it can be said that an approximate average increase of heat flux for Ethanol is about 30% higher than Methanol and 150% higher than Acetone.

Fig 2(d) shows the effect of different geometries on Ethanol (without fan). Rectangular Finned Surface (RFS) showed better heat transfer than that of Pin Finned Surface (RFS) and Plain Surface (PS). With RFS, the achieved average heat flux is about 30 % higher than plain surface and about 15 % higher than pin fin surface.

3 Effects of Fan on Heat Flux for Working Fluids with Different Geometries

A condensing fan of 40 Watt was employed for creating the forced convection effect in condenser. Boiling curves for plain surface PS for Methanol, Ethanol and Acetone with and without fan are given in the Figs. 3 (a-c). In each curve higher heat flux is obtained by using fan. From Fig. 3(a) it is found that while using fan heat fluxes are reduced slightly within $\Delta T = 8\text{-}10^{0}$ C. After that temperature, heat flux increases again and reaches up to around 90 kW/m^2. Heat flux also increases with wall super heat for Ethanol (Fig. 3 (b)) and Acetone (Fig. 3 (c)). For all the cases, the value of heat flux (with and without fan) becomes closer as the wall superheat increases.

More high heat flux is corresponding to high wall superheat. At higher heat flux the condenser becomes heated also and consequently the temperature gradient between the condenser surface and atmosphere becomes high which results in high heat transfer from the condenser to the atmosphere naturally (without fan). As the condenser temperature increases (resulted from high test surface heat flux), the force convection effect by the fan starts becoming relatively less effective with respect to natural convection (without fan). Therefore, with the increase of wall superheat, the heat flux with and without fan becomes closer.

Boiling curves of pin fin surface (PFS) for Methanol, Ethanol and Acetone with and without fan are given in the Fig. 4. In these curves, higher heat flux is obtained for Ethanol. From Fig. 4(b) with fan, the maximum obtained heat flux for Ethanol is about 100 kW/m^2.

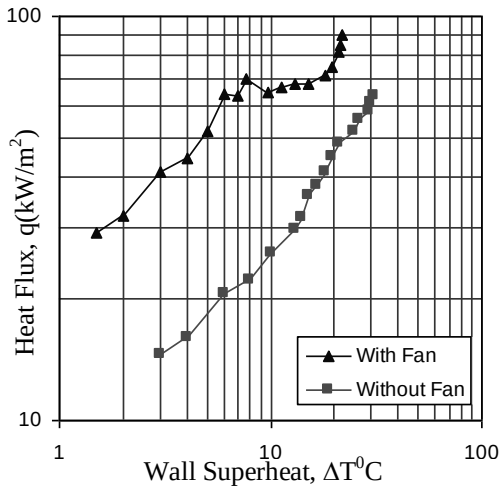

(a) Methanol

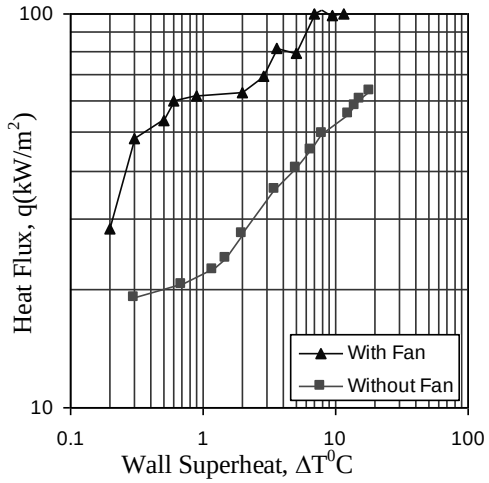

(b) Ethanol

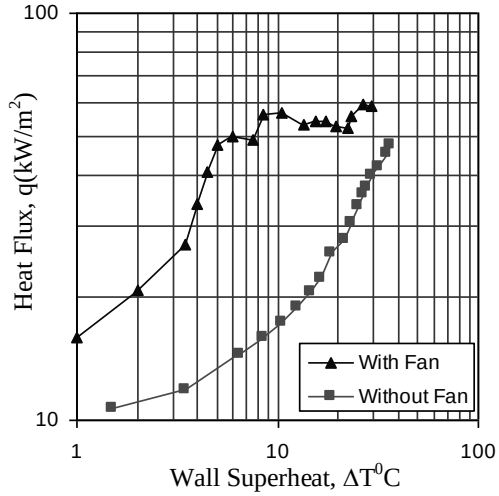

(c) Acetone

Fig. 3 Effects of fan on heat flux (Plain Surface, PS)

In Figs. 3 -4, just after the wall superheat of (8-10) ^{o}C, the heat flux decreases a bit for most of the cases. It might be explained in the way that, in this region of wall superheat, fan decreased the liquid temperature below the corresponding temperature of the most vigorous nucleate boiling. With the increase of wall superheat (i e. with the increase of solid surface temperature), the flowing liquid temperature increases and the fan is then not capable to reduce the liquid temperature below the corresponding of vigorous boiling temperature.

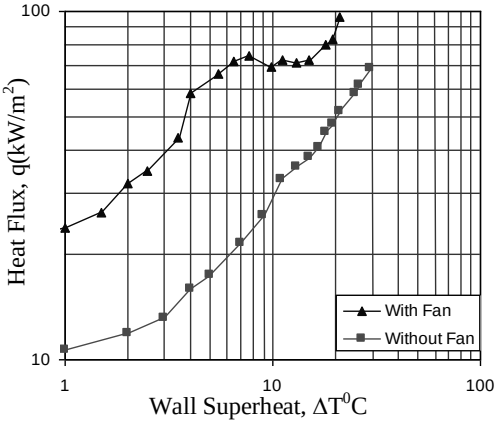

(a) Methanol

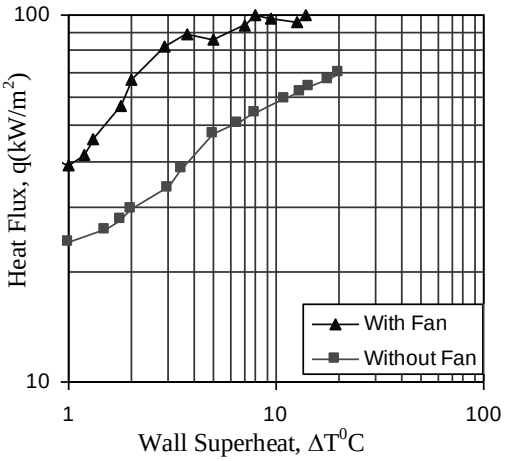

(b) Ethanol

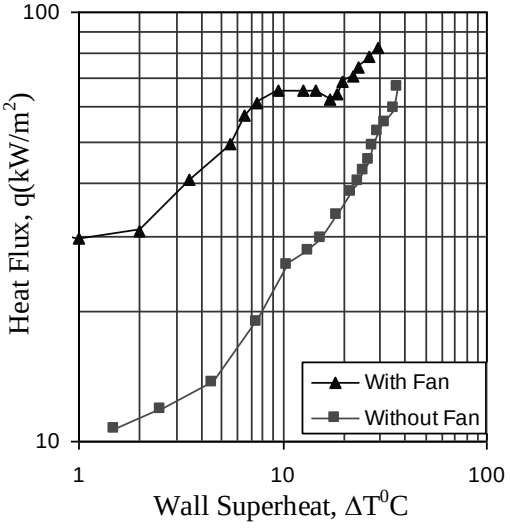

(c) Acetone

Fig. 4 Effects of fan on heat flux (Pin Finned Surface, PFS)

Boiling curves of Rectangular Fin Surface, RFS for Methanol, Ethanol and Acetone with and without fan are given in the Fig. 5. In these curves higher heat flux is also obtained for Ethanol. From Fig. 5(b) with fan, the achieved maximum heat flux for Ethanol is 110 kW/m^2. For Methanol and Acetone the obtained maximum heat fluxes are found 96 kW/m^2 and 82 kW/m^2 , respectively from Figs. 5(a) and (c). In Fig. 5(a) Methanol with fan shows steeper slope initially than without fan at i.e. rate of increase of heat flux is higher for smaller wall superheat. For higher wall superheat, the heat flux becomes less steep with wall superheat. It can be explained with typical boiling phenomena. Boiling heat flux is the maximum at nucleate boiling and more or less at certain wall superheat range. If the wall superheat becomes higher than the wall superheat corresponding to nucleate boiling (or the maximum heat flux), a vapor blanket starts forming between the solid and the liquid which results in reduction of heat flux with the increase of wall super heat.

Employing condenser fan always produces better heat transfer than that of without fan. More or less 150% average heat flux can be increased by employing a fan of 40 Watt.

4 Effects of Bubble Frequency(f_b) and Surface Geometries on Heat Flux

Heat flux,q vs Bubble frequency,f_b graph for surface PS, PFS and RFS of Methanol at different temperatures (80^oC, 83^oC and 86^oC) with and without fan are given in the Figs. 6. In these graphs, it is found that RFS produces higher heat flux than PFS and PS. PFS produces more heat flux than PS. Heat flux increases with bubble frequency. For RFS, the maximum obtained heat flux is estimated to 59 kW/m^2 and 96 kW/m^2 at 86^0C for without and with fan respectively. Bubble generation frequency, f_b is the number of bubbles generated per second from a particular point on the bubble generating surface. Higher rate of bubble generation frequency means higher rate of heat carried from the hot surface to the surrounding liquid. A single bubble takes a particular amount of heat, so when the number of bubble generation per unit time increases, the amount of heat transfer naturally increases.

Heat flux vs. bubble frequency for PS, PFS and RFS for Ethanol at different temperatures with and without fan are given in the Fig. 7. In these graphs, it is found that RFS produces higher heat flux than PFS and PS. PFS produces more heat flux than PS. Heat flux increases with bubble frequency. For RFS, the maximum obtained heat flux is estimated to 60 kW/m^2 (without fan) and 105 kW/m^2 (with fan) at 86^0C for evaporator surface temperature. Nucleate boiling is mainly responsible for higher heat flux. On the other hand, bubble nucleation depends on the surface geometry and the number of sites for entrapped gas. The rectangular fin geometry (RFS) is such that there exists the highest number of cavities for entrapped gas which consequences the maximum heat flux. The entrapped gas cavities and the heat flux decreases for pin fin geometry (PFS). The plain surface (PS) contains the minimum number of cavities which results in the minimum heat flux among the three surfaces.

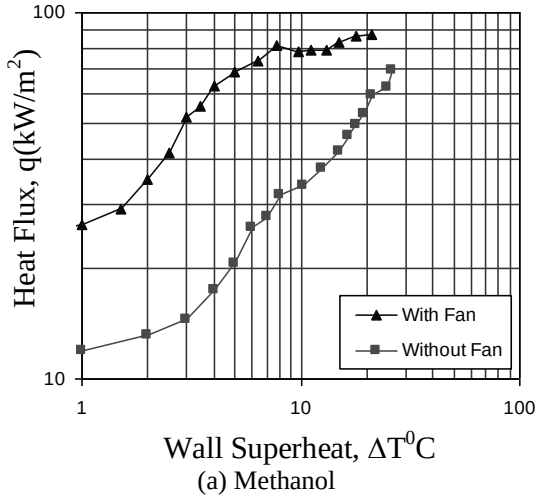

(a) Methanol

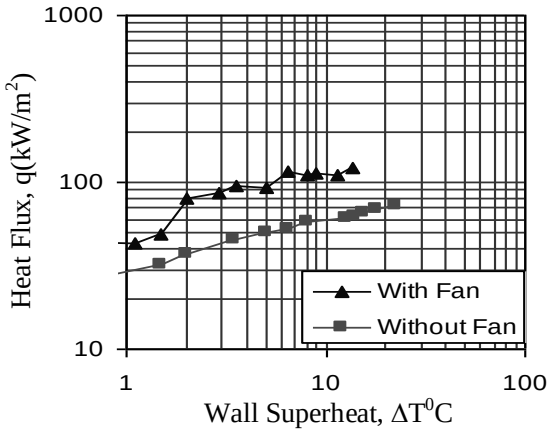

(b) Ethanol

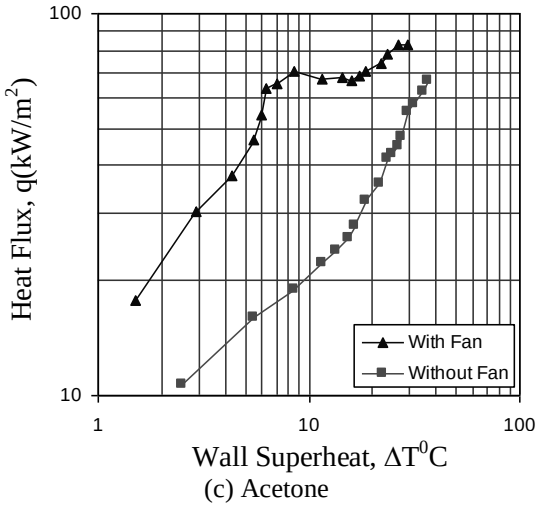

(c) Acetone

Fig. 5: Effects of fan on heat flux (Rectangular Finned Surface, RFS)

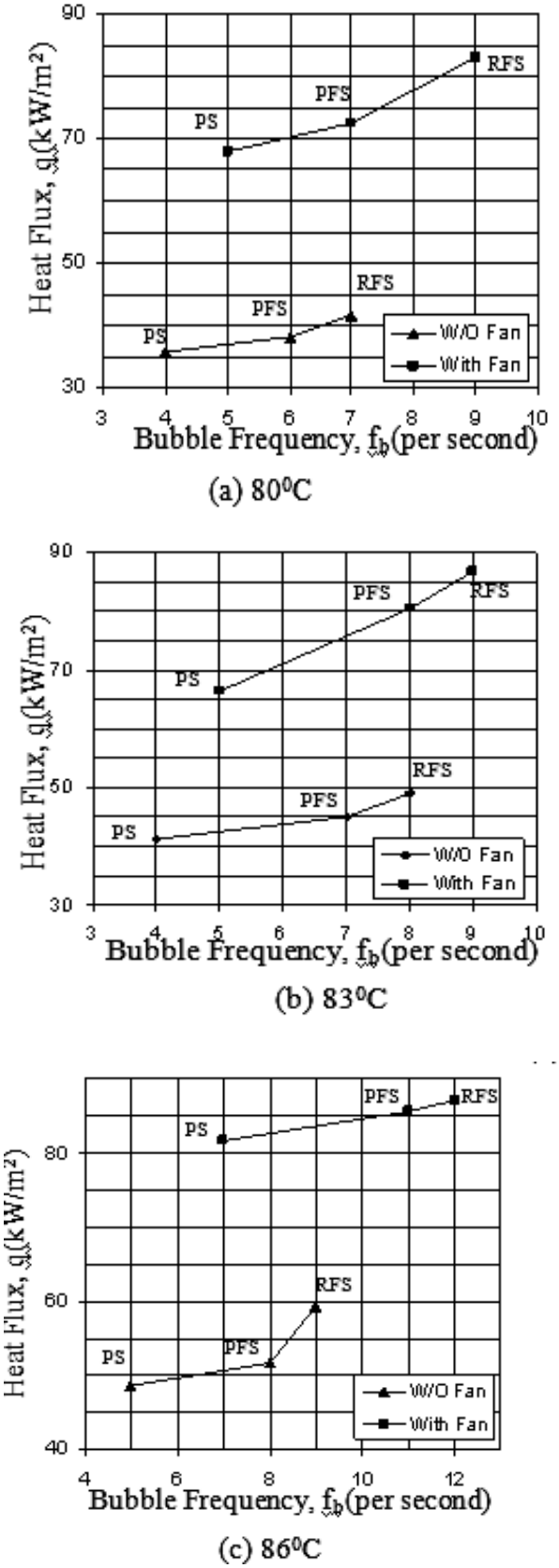

Fig. 6 Effects of bubble frequency on heat flux (Methanol)

Heat flux vs. bubble frequency graph for PS, PFS and RFS for Acetone at different temperatures with and without fan are given in the Fig. 8. In this graph, it is also found that RFS produces higher heat flux than PFS and PS. PFS produces more heat flux than PS. It is also found here that heat flux increases with bubble frequency. For RFS, the maximum heat flux is estimated to 55 kW/m^2 (without fan) and 82 kW/m^2 (with fan) at 86^{0}C.

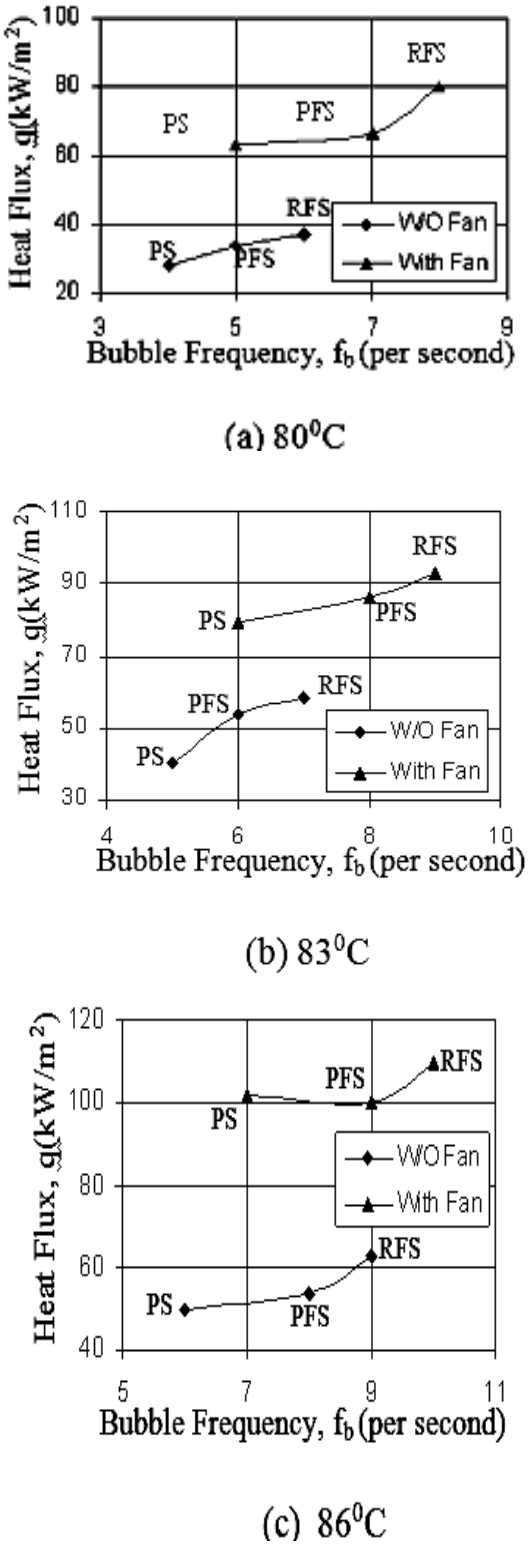

Fig. 7 Effects of bubble frequency on heat flux (Ethanol)

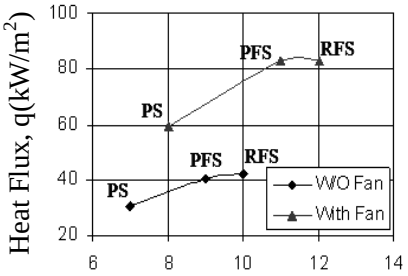

(a) 80^0C

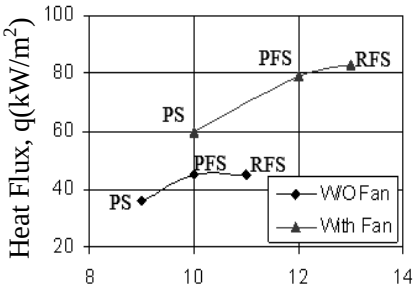

(b) 83^0C

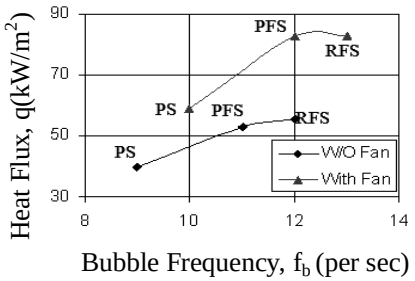

(c) 86^0C

Fig. 8 Effects of bubble frequency on heat flux (Acetone)

5 Variation of Heat Flux with Bubble Density

Heat flux vs bubble density per cm^2 graph for PS, PFS and RFS of three working fluids at different temperatures (80^oC, 83^oC and 86^oC) with fan are given in the Fig. 9. In Fig. 9(a), RFS with Methanol produces maximum heat flux of about 84 kW/m^2 at $80\ ^0C$. From Figs. 9 it is found that RFS with Ethanol at 86^0C has the highest heat flux of about 109 kW/m^2. Although Acetone has high bubble density than Methanol and Ethanol, due to its less bubble frequency heat flux is lower. Actually heat flux is a function of the product of bubble generation frequency and bubble density per unit area.

Heat flux vs. bubble density for PS, PFS and RFS of three working fluids at different temperatures without fan are given in the Fig. 10. In Fig. 10(a) at 80^0C it is shown that Acetone has higher bubble density and higher heat flux. Methanol produces increased heat flux as high as 42 kW/m^2 with RFS. For Acetone also, heat flux increases with bubble density. For 80 ^oC of solid surface temperature, acetone has the highest wall superheat among the three (as the saturated temperature of acetone is the lowest). This wall superheat might be suitable for nuclear boiling (higher heat flux) for acetone which consequences of higher generation of bubble per unit area and results in higher heat flux. Actually heat flux may not linearly proportional to the bubble density which is found from the curves shown in the Figs. 10 (a), (b)

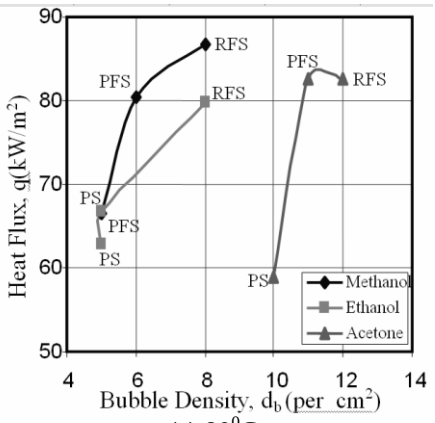

(a) 80^0C

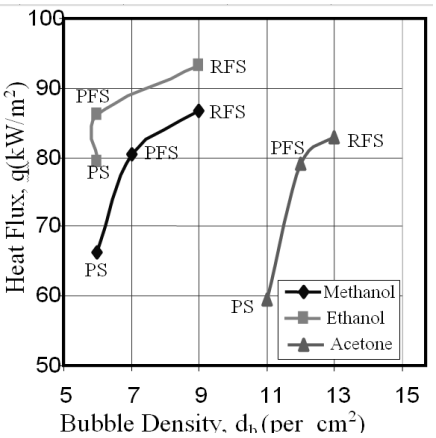

(b) 83^0C

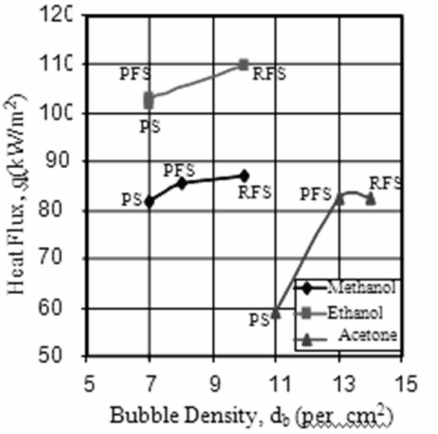

(c) 86^0C

Fig. 9 Heat flux and bubble density for different geometries (with fan)

and (c). A bubble may be superheated or saturated and many other parameters are involved for the amount of heat carried by a single bubble. Therefore, heat flux should not be always directly proportional to the bubble density.

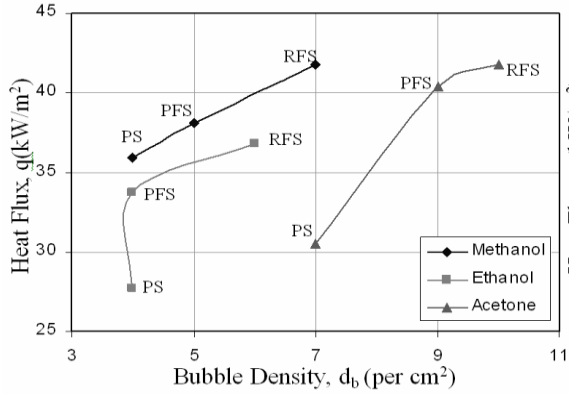

(a) 80^0C

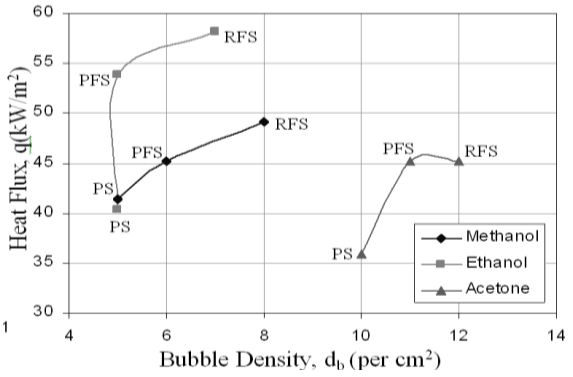

(b) 83^0C

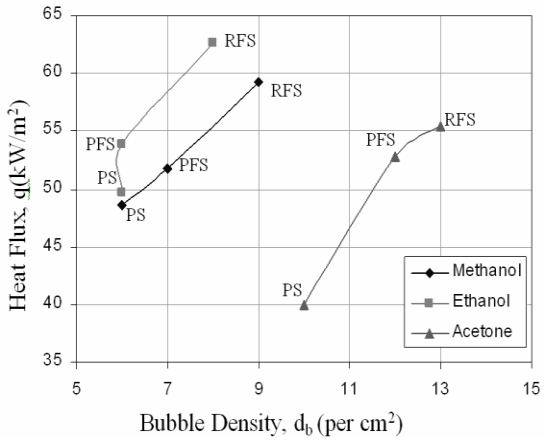

(c) 86°C

Fig. 10 Variation of heat flux and bubble density on working fluids for different geometries (without fan)

6 Visual Observations of Bubble Generation Characteristics

Photographic images of bubble generation at different experimental conditions are described in this section (Figs. 11-12). For same experimental condition (surface temp: 86°C, Ethanol, without fan), RFS shows highly dense bubble generation (f_b = 9/sec d_b = 8/cm^2) as represented in Fig. 11. The rectangular geometry is such that there is always a chance for creating more vapor bubbles. The rectangular geometry is responsible for trapping much amount of air which is ultimately produces more bubble during heating. The heat flux for RFS is also maximum here compared to PFS and PS. A very rough assumption may be considered here, like, the product of f_b and d_b is an indication of heat flux. This value is 9x8 = 72 here for RFS, which are 48 and 36 for PFS and PS. The heat flux follows the value of this product at least for a significant number of experimental conditions in this study.

The effect of bubble generation frequency and density with evaporator surface temperature is represented in Fig. 12. From the photograph, it seems that at 86 °C the bubble generation rate is the maximum among the three temperatures. The product of f_b and d_b is 9x8 = 72 for the temperature 86 °C and this value is 36 and 49 for 80 °C and 83 °C of the evaporator surface temperature. This phenomenon reveals that with the increase of surface temperature, the rate of bubble generation increases at least for the mentioned temperature range (it is to be mentioned here that the evaporator surface temperature around 80-86 °C has been considered here due to the cause that most of the electronic devices run in this range).

The boiling temperature of Ethanol at atmospheric pressure is about 78.3 °C. Another visual observation for bubble generation for a particular temperature (83 °C) and time (0.22 sec) with the variation of liquid is shown in Fig. 13. The figure reveals that acetone shows the most dense bubble generation. The boiling temperature T_b at atmospheric pressure is 56.3 °C for acetone (it is the lowest T_b among all the three; T_b for methanol is 64.5 °C and that for ethanol is 78.3 °C). In this sense, the wall superheat for acetone is 83°C – 56.3 °C = 26.7 °C which is the highest among all the fluids. Among all the experimental conditions, Acetone falls in the most favorable wall superheat condition corresponding to generation of maximum number of bubbles. This consequences higher rate of bubble generation for acetone.

7 Comparison of Experimental Results

The experimental heat fluxes with ethanol as working fluid have been compared with the experimental results with ethanol obtained by Mahmood et al. (2008). The Smooth Surface (SS) heat flux from Mahmood et al. is comparable with that of the Plain Surface (PS) from the present study as shown in Fig. 14. On the other hand, the heat flux of the present study with Rectangular Fin Surface (STRS) from Mahmood et al. (2008). Therefore, it can be said that a good agreement is found between the experimental results of the present study with that of obtained by Mahmood et al (2008).

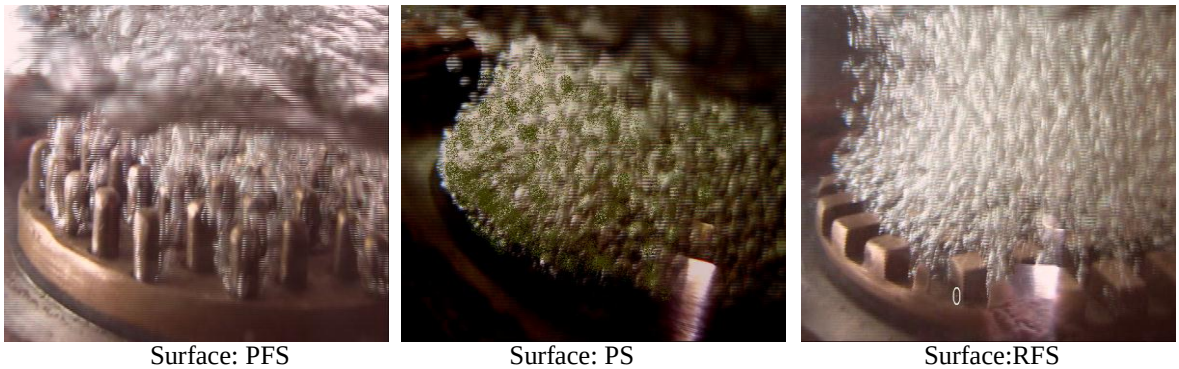

Surface: PFS f_b=8/sec, d_b=6/cm^2 | Surface: PS f_b=6/sec, d_b=6/cm^2 | Surface:RFS f_b=9/sec, d_b=8/cm^2

Fig 11 Photograph of Ethanol with Different Geometry, Surface Temp. 86 ^{o}C (w/o fan)

80^0C f_b=6/sec, d_b=6/cm^2 | 83^0C f_b=7/sec, d_b=7/cm^2 | 86^0C f_b=9/sec, d_b=8/cm^2

Fig 12 Photographic View of Ethanol with Geometry RFS at 80^0C, 83^0C and 86^0C

Working Fluid: Methanol | Working Fluid: Ethanol | Working Fluid: Acetone

Fig 13 Photograph of Rectangular Finned Surface (RFS) at 83^0C and at 0.22 sec(with fan)

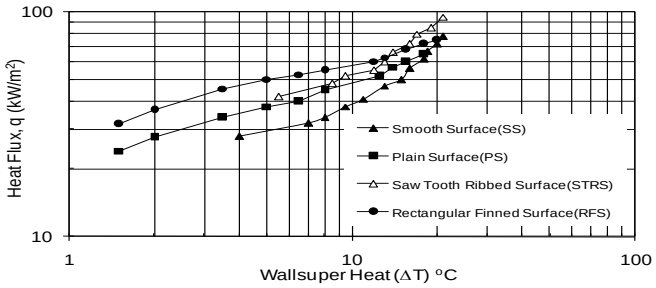

Fig 14 Comparison of experimental heat flux from the present study with Mahmood et al. (2008) (working fluid Ethanol)

4. CONCLUSIONS

Phase change during boiling makes the thermal and hydrodynamic characteristics of thermosyphon more complicated. The following accomplishments may be summarized at the moment:

- Surface geometry has immense effect on the heat transfer rate. Rectangular Finned Surface (RFS) has showed better heat transfer than that of Pin Finned Surface (PFS) and Plain Surface (PS). With RFS, the achieved average heat flux is about 30% higher than plain surface and 15 % higher than pin fin surface.
- Choice of working fluid has an important impact on heat flux. Ethanol showed the highest heat flux for a particular experimental condition among methanol, ethanol and acetone. The average increase of heat flux for ethanol is about 30 % higher than methanol and about 150 % higher than acetone.
- Average heat flux by using condensing fan can be increased up to 150 % at the cost of 40 W energy consumption due to fan.
- There is a definite impact of bubble frequency per second on heat flux. Experiment shows that heat flux increases with bubble frequency.
- Bubble density per unit area has also immense effect on heat flux. Bubble density increases with surface temperature that resulted better heat flux.

REFERENCES

Bernier M.A., Baliga B.R. 1992. A 1-D/2-D model and experimental results for a closed-loop thermosyphon with vertical heat transfer sections", International Journal of Heat and Mass Transfer, 35, 2969-2982

Charles C.J.V., Kok, J.B.W. 1992. Investigation of the overall transient performance of the industrial two-phase closed loop thermosyphon, International Journal of Heat and Mass Transfer, 35, 1419-1426

Claudio, C., Flavio, D. 1988. Experimental investigation and analytical modeling of a closed two-phase thermosyphon with imposed convection boundary conditions, International Journal of Heat and Mass Transfer, 31, 1815-1833

Fichera, A.P. 2002. Neural network-based prediction of the oscillating behaviour of a closed loop thermosyphon , International Journal of Heat and Mass Transfer, 45, 3875-3884

Gavotti, N., Polasek, F. 1999. Thermal Control of Electronics Components by Two-Phase Thermosyphons, Proceedings of Eurotherm Seminal, No. 63

Gross U., Hahne E. 1985. Instability and unproportional pressure variations near the thermodynamic critical point in a closed thermosyphon, International Journal of Heat and Mass Transfer, 28, 1551-1561

Ghiu, C.D., Joshi, Y.K., Nakayama, W., 2001, "Visualization study of pool boiling from transparent enhanced structures", Proceedings of the National Heat Transfer Conference, Anaheim, CA, 1, 697-704

Hasanuzzaman, M., Saidur, R., Ali, M., Masjuki, H.H. 2007. Effects of variables on natural convective heat transfer through V-corrugated vertical plates, International Journal of Mechanical and Materials Engineering, 2(2), 109-117

Imura H., Sasaguchi K., Kozai, H. 1983. Critical Heat flux in a closed two phase thermosyphon, Int. J. of heat and Mass Transfer, 26,1181-1188

Lang, Y.J.Y., Nakayama, W. 2001. Effect of Condenser Location and Tubing Length on the Performance of a Compact Two-Phase Thermosyphon", Proceedings of 2001 Int. Mechanical Engineering Congress and

Lee, Y., Mital, U. 1972. A two-phase closed thermosyphon", International Journal of Heat and Mass Transfer, 15, 1695-1707

Mahmood S.L., Bagha N., Akhanda, M.A.R., Islam, A.K. M.S. 2008. Heat Transfer Characteristics inside an Evaporator of a Two-Phase Closed Loop Thermosyphon with Saw Tooth Ribbed Evaporator Surface, Advanced Design and Manufacture to Gain a Competitive Edge, Book Author: Yan, Xiu-Tian, Jiang, Chengyu, Eynard, Benoit, Publisher: Springer-London, 1st Edition, ISBN 9781848002418, 111-120

Mark, A.C., Christopher, R.Y., Kim C.N. 2009. Modeling and testing of an advanced compact two-phase cooler for electronics cooling", Int. Journal of Heat and Mass Transfer, 52, 3456-3463

Mughal M.P., Plumb O.A. 1996. An experimental study of boiling on a wicked surface, International Journal of Heat and Mass Transfer, 39, 771-777

Ramaswamy, C., Joshi, Y., Nakayama, W. 1998, "Performance of a Compact Two-Chamber Two-Phase Thermosyphon: Effect of Evaporator Inclination, Liquid Fill Volume and Contact Resistance", Proc. Of the 11th International Heat Transfer Conference, Kyongju, South Korea, 2, 127-132

Ramos E., Sen M., Trevino C. 1985. A steady-state analysis for variable area one- and two-phase thermosyphon loops, International Journal of Heat and Mass Transfer, 28, 1711-1719

Yinxue, S. Zhongqi, C. 1995. 2-D numerical study on a rectangular thermosyphon with vertical or horizontal heat transfer sections, International Journal of Heat and Mass Transfer, 38, 3313-33